

First-principles study of constitutional and thermal point defects in B2 PdIn

Chao Jiang^{a,*}, Long-Qing Chen^b, Zi-Kui Liu^b

^aDepartment of Materials Science and Engineering, Iowa State University, 3308 Gilman Hall, Ames, IA 50011, USA

^bDepartment of Materials Science and Engineering, The Pennsylvania State University, University Park, PA 16802, USA

Received 5 January 2005; accepted 31 May 2005

Available online 9 August 2005

Abstract

We performed first-principles calculations to investigate the point defect structure of B2 PdIn. In agreement with experiments, our calculations show that Pd vacancies and Pd antisites are the constitutional point defects in In-rich and Pd-rich B2 PdIn, respectively. To predict the thermal defect concentrations at finite temperatures, we adopted the statistical-mechanical Wagner–Schottky model in combination with our first-principles calculated point defect formation enthalpies. Our calculations suggest that the predominant thermal defects in B2 PdIn are of triple-defect type and not of Schottky type.

© 2005 Elsevier Ltd. All rights reserved.

Keywords: A. intermetallics, miscellaneous; D. defects: point defects; E. ab initio calculations; E. defects: theory

1. Introduction

The intermetallic compound PdIn dominates the central part of the In–Pd phase diagram with its wide homogeneity range [1]. It is a 3:2-type electron compound with a strongly ordered B2 (CsCl-type) structure and remains ordered up to its melting point at 1285 °C. Its B2 structure consists of two interpenetrating simple cubic sublattices, with each sublattice having equal number of lattice sites. In its perfectly ordered state at the stoichiometric composition, one sublattice is entirely occupied by In and the other entirely by Pd atoms. Deviations from the ideal stoichiometry are accommodated by the formation of constitutional (structural) point defects. Interestingly, like in B2 NiAl [2], the constitutional point defects in B2 PdIn are of different type on different side of stoichiometry: Pd vacancies on In-rich side and Pd antisites on Pd-rich side [3–5]. The existences of those point defects have profound effects on such important properties of B2 alloys as mechanical properties and diffusion mechanisms [6–8].

At finite temperatures, thermal defects will also be activated in addition to the constitutional ones by entropy.

Since single point defects in ordered alloys alone are not composition-conserving, those thermal defects have to appear in balanced combinations in order to maintain the overall composition of the alloy. From their lattice parameter and bulk density measurements, Huang et al. [9,10] obtained the vacancy concentrations in B2 PdIn as a function of alloy composition at various temperatures. Based on the observation that their data can be fitted quite well by the equation derived for triple-defect type B2 alloys by Chang and Neumann [5], they concluded that the thermal defects in B2 PdIn are of triple-defect type, i.e. simultaneous creation of two Pd vacancies and one Pd antisite. The triple-defect model has been adopted to describe the B2 PdIn phase in a thermodynamic modeling of the In–Pd binary system by Jiang and Liu [11] using the CALPHAD (Calculation of Phase Diagrams) approach. However, using perturbed angular correlation of gamma rays (PAC) technique, Collins and Shiha [12] observed vacancies on both the In and Pd sublattices in about equal amounts and thus argued that the thermal defects in B2 PdIn are of Schottky type, i.e. simultaneous creation of one In vacancy and one Pd vacancy.

Based on density functional theory (DFT) [13], first-principles calculations have now been routinely used to predict properties of a wide range of materials. These methods are truly predictive since only atomic numbers and crystal structure information are needed as inputs. In view of

* Corresponding author. Tel.: +1 515 294 0739; fax: +1 515 294 5444.
E-mail address: chaoisu@iastate.edu (C. Jiang).

the experimental controversies, it is thus highly desirable to use first-principles calculations to provide some insight, which is the goal of the present paper.

2. Computational methodology

2.1. Mean-field formalism

In studying the point defect structure of B2 PdIn, it is assumed that those point defects are sufficiently dilute, which allows us to adopt the Wagner–Schottky model (a gas of non-interacting point defects on well-defined sublattices) [14–16] to calculate the point defect concentrations as a function of alloy composition and temperature. Instead of using a grand-canonical ensemble (i.e. a fixed number of lattice sites with varying number of atoms), here we consider a canonical ensemble containing a fixed number of In and Pd atoms and the total number of lattice sites may thus vary when vacancies are present. In this case, it is more convenient to use the atomic concentration rather than the site fraction [15]. The atomic concentration of species i on sublattice α is defined as:

$$x_{i_\alpha} = \frac{n_{i_\alpha}}{N_{\text{atom}}} \quad (1)$$

where N_{atom} is the total number of atoms (thus excluding vacancies) and n_{i_α} is the number of species i on the α sublattice with $i = \{\text{In, Pd, Va}\}$ and $\alpha = \{\text{In, Pd}\}$. Here Va denotes vacancy.

According to the Wagner–Schottky model, the formation enthalpy (per atom) of a B2 PdIn alloy is a linear function of the point defect concentrations:

$$\Delta H = \Delta H_{\text{PdIn}} + \sum_d H_d x_d \quad (2)$$

where x_d is the atomic concentration of defects of type d with $d = \{\text{Va}_{\text{Pd}}, \text{Va}_{\text{In}}, \text{Pd}_{\text{In}} \text{ and } \text{In}_{\text{Pd}}\}$. ΔH_{PdIn} is the formation enthalpy of the fully-ordered stoichiometric B2 PdIn and H_d is the formation enthalpy of isolated point defects of type d in stoichiometric B2 PdIn, which will be obtained in the present study through first-principles calculations.

In considering the effects of finite temperatures, the effects of vibrational entropies will be neglected and the configurational entropy (per atom) will be treated using the following mean-field approximation:

$$S = k_B (1 + x_{\text{Va}_{\text{In}}} + x_{\text{Va}_{\text{Pd}}}) \ln \left(\frac{1 + x_{\text{Va}_{\text{In}}} + x_{\text{Va}_{\text{Pd}}}}{2} \right) - k_B \sum_\alpha \sum_i x_{i_\alpha} \ln(x_{i_\alpha}) \quad (3)$$

where the summation goes over $i = \{\text{In, Pd, Va}\}$ and $\alpha = \{\text{In, Pd}\}$. k_B is the Boltzmann's constant.

The equilibrium concentrations of point defects can now be obtained through a minimization of the Gibbs free energy

of the system, i.e. $\Delta G = \Delta H - TS = \min$, which together with the mass-balance constraints leads to the following set of non-linear equations:

$$\frac{2x_{\text{Va}_{\text{In}}}x_{\text{In}_{\text{Pd}}}}{x_{\text{Va}_{\text{Pd}}}(1 - 2x_{\text{Pd}_{\text{In}}} - x_{\text{Va}_{\text{In}}} + x_{\text{Va}_{\text{Pd}}})} = \exp \left[-\frac{H_{\text{In}_{\text{Pd}}} - H_{\text{Va}_{\text{Pd}}} + H_{\text{Va}_{\text{In}}}}{k_B T} \right] \quad (4a)$$

$$\frac{2x_{\text{Va}_{\text{Pd}}}x_{\text{Pd}_{\text{In}}}}{x_{\text{Va}_{\text{In}}}(1 - 2x_{\text{In}_{\text{Pd}}} + x_{\text{Va}_{\text{In}}} - x_{\text{Va}_{\text{Pd}}})} = \exp \left[-\frac{H_{\text{Pd}_{\text{In}}} + H_{\text{Va}_{\text{Pd}}} - H_{\text{Va}_{\text{In}}}}{k_B T} \right] \quad (4b)$$

$$\frac{4x_{\text{Va}_{\text{In}}}x_{\text{Va}_{\text{Pd}}}}{(1 + x_{\text{Va}_{\text{In}}} + x_{\text{Va}_{\text{Pd}}})^2} = \exp \left[-\frac{H_{\text{Va}_{\text{In}}} + H_{\text{Va}_{\text{Pd}}}}{k_B T} \right] \quad (4c)$$

$$\frac{1}{2}(1 - 2x_{\text{In}_{\text{Pd}}} + 2x_{\text{Pd}_{\text{In}}} + x_{\text{Va}_{\text{In}}} - x_{\text{Va}_{\text{Pd}}}) = x_{\text{Pd}} \quad (4d)$$

where x_{Pd} is the total mole fractions of Pd in the alloy. A numerical solution of Eq. (4a)–(4d) can thus give us the equilibrium concentrations of all point defects at a given alloy composition and temperature.

2.2. First-principles methods

In the present study, a first-principles supercell approach was employed to obtain the formation enthalpies of isolated point defects in stoichiometric B2 PdIn. Such an approach has been widely used in the literature for studying defects in materials [15–25]. Here we used both a 16-atom $2 \times 2 \times 2$ cubic B2 supercell and a larger 32-atom supercell [17], each containing one single point defect (vacancy or antisite) per supercell. The periodically arranged point defects in 16-atom supercells form a simple-cubic lattice with a lattice parameter of $2a$, while the point defects in 32-atom supercells form a fcc lattice with a lattice parameter of $4a$. Here a is the B2 lattice parameter. The lattice vectors and atomic positions of the 32-atom supercell in its ideal, unrelaxed form are given in Table 1, all in Cartesian coordinates.

First-principles calculations were performed using the plane wave method with Vanderbilt ultrasoft pseudopotentials [26,27], as implemented in the highly-efficient Vienna ab initio simulation package (VASP) [28,29]. We employed the local density approximation (LDA) with the exchange-correlation functional from Ceperley and Alder [30]. The semi-core $4d$ electrons of In were explicitly treated as valence. The k -point meshes for Brillouin zone sampling were constructed using the Monkhorst–Pack scheme [31] and the total number of k -points times the total number of atoms per unit cell was at least 10000 for all structures. A plane wave cutoff energy of 248.7 eV was used. All calculations included scalar relativistic corrections (i.e. no spin-orbit interaction).

Table 1
Structural description of the 32-atom $A_{15}B_1C_{16}$ supercell

Lattice vectors	$\vec{a}_1 = (2.0, 0.0, -2.0)$, $\vec{a}_2 = (2.0, -2.0, 0.0)$, $\vec{a}_3 = (0.0, -2.0, -2.0)$
Atomic positions	A - (2.5, -1.5, -2.5), A - (2.5, -2.5, -1.5), A - (1.5, -1.5, -1.5), A - (2.5, -1.5, -1.5), A - (3.5, -3.5, -3.5), A - (1.5, -0.5, -1.5), A - (2.5, -2.5, -3.5), A - (1.5, -1.5, -0.5), A - (2.5, -3.5, -2.5), A - (0.5, -0.5, -0.5), A - (1.5, -2.5, -2.5), A - (2.5, -2.5, -2.5), A - (1.5, -1.5, -2.5), A - (1.5, -2.5, -1.5), A - (0.5, -1.5, -1.5), B - (3.5, -2.5, -2.5), C - (3.0, -3.0, -3.0), C - (2.0, -2.0, -3.0), C - (2.0, -3.0, -2.0), C - (1.0, -2.0, -2.0), C - (2.0, -2.0, -2.0), C - (3.0, -2.0, -2.0), C - (3.0, -3.0, -2.0), C - (3.0, -3.0, -2.0), C - (2.0, -1.0, -2.0), C - (3.0, -2.0, -3.0), C - (2.0, -2.0, -1.0), C - (4.0, -3.0, -3.0), C - (1.0, -1.0, -1.0), C - (2.0, -3.0, -3.0), C - (3.0, -4.0, -3.0), C - (3.0, -3.0, -4.0), C - (4.0, -4.0, -4.0)

Lattice vectors and atomic positions are given in Cartesian coordinates, in units of a , the B2 lattice parameter. Atomic positions are given for the ideal, unrelaxed B2 sites.

As the initial step, the unit cell volumes of all structures were fully relaxed with all atoms occupying their ideal lattice positions. To further consider the effects of local atomic relaxations around point defects, we then fully relaxed all the atoms from their ideal lattice sites into their equilibrium positions according to the quantum-mechanical Hellmann-Feynman forces using a Quasi-Newton algorithm, maintaining the overall volume and shape of the unit cell. After relaxations, the forces acting on the atoms are less than 0.01 eV/Å.

The formation enthalpies of $In_{1-x}Pd_x$ alloys can be calculated from the following equation:

$$\Delta H(In_{1-x}Pd_x) = E(In_{1-x}Pd_x) - (1-x)E(In) - xE(Pd) \quad (5)$$

where $E(In)$, $E(Pd)$ and $E(In_{1-x}Pd_x)$ are the first-principles calculated total energies (per atom) of the constituent pure elements In and Pd and the corresponding alloy, respectively, each relaxed to their equilibrium geometries. Here x is the molar composition of Pd in the alloy. Body-centered tetragonal (bct) In and fcc Pd were used as reference states in Eq. (5).

Finally, we obtain the formation enthalpies of point defects by means of finite differencing, as follows [32]:

$$H_d = \frac{\partial \Delta H}{\partial x_d} \approx \frac{\Delta H_d - \Delta H_{PdIn}}{x_d} \quad (6)$$

where ΔH_d is the formation enthalpy (per atom) of a 16-atom (32-atom) B2 PdIn supercell containing one point defect of type d and ΔH_{PdIn} is the formation enthalpy of

perfectly ordered defect-free B2 PdIn. For the 16-atom supercells, we have $x_d = 1/16$ for antisites and $x_d = 1/15$ for vacancies. For the 32-atom supercells, we have $x_d = 1/32$ for antisites and $x_d = 1/31$ for vacancies.

In our calculations, we used a $9 \times 9 \times 9$ k -point mesh for the 16-atom B2 supercells and a $8 \times 8 \times 8$ k -point mesh for the 32-atom supercells, which correspond to 35 and 29 irreducible k -points in the Brillouin zone, respectively. Our convergence tests showed that those k -point meshes were sufficient to give fully converged results. The final results are given in Table 2. As shown, in our unrelaxed calculations, the results obtained using 32-atom supercells are very similar to those obtained using 16-atom supercells. The defect formation enthalpies however have a stronger dependence on supercell size when the effects of local atomic relaxations are taken into account. This is due to the fact that larger supercells have larger degrees of freedom for relaxation, which thus leads to larger decreases in defect formation enthalpies due to local atomic relaxations. The fully relaxed point defect formation enthalpies obtained using 32-atom supercells are used in the following calculations.

3. Results and discussions

3.1. Lattice parameters of pure elements

To determine the equilibrium c/a ratio of bct In, we calculated the total energy of In along the tetragonal transformation path and the results are shown in Fig. 1.

Table 2
First principles calculated formation enthalpies (eV/defect) of isolated point defects and complex composition-conserving defects in stoichiometric B2 PdIn

Defect type	Designation	16-atom supercell		32-atom supercell	
		Unrelaxed	Relaxed	Unrelaxed	Relaxed
Pd vacancy	V_{apd}	0.54	0.46	0.50	0.41
In Antisite	In_{pd}	2.45	2.07	2.53	2.01
In vacancy	V_{ain}	1.13	1.12	1.02	0.87
Pd Antisite	Pd_{in}	0.36	0.34	0.31	0.11
Triple Pd	$0 \rightarrow 2V_{apd} + Pd_{in}$	1.44	1.26	1.31	0.93
Schottky	$0 \rightarrow V_{apd} + V_{ain}$	1.67	1.58	1.52	1.28
Exchange	$0 \rightarrow In_{pd} + Pd_{in}$	2.81	2.41	2.84	2.12
Triple In	$0 \rightarrow 2V_{ain} + In_{pd}$	4.71	4.31	4.57	3.75

Both unrelaxed (volume relaxations only) and fully relaxed (volume + local atomic relaxations) values are shown. Reference states: bct In and fcc Pd.

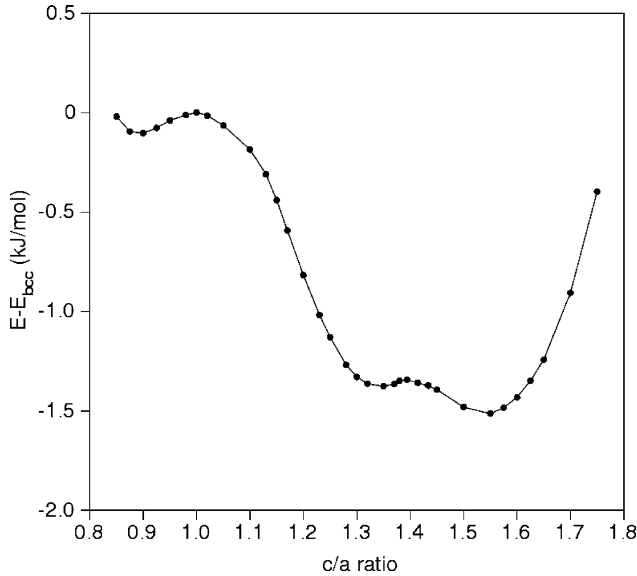


Fig. 1. Total energy of In along the tetragonal transformation path with respect to E_{In}^{bcc} . The volume is fully relaxed at each c/a ratio.

Interestingly, there are actually three bct structures with different $c/a\sqrt{2}$ ratios (one with $c/a < 1$, one with $1 < c/a < \sqrt{2}$, and one with $c/a > \sqrt{2}$), as manifested by the three minima in Fig. 1. Such a behavior has also been reported in previous first-principles studies by Simak et al. [33] and Mikhaylushkin et al. [34]. The global minimum in Fig. 1 corresponds to the ground-state bct structure of In at zero pressure. Our first-principles calculated equilibrium lattice parameters of bct In and fcc Pd are given in Table 3. The calculated c/a ratio of In agrees well with experiments. The calculated lattice parameters of In and Pd are 1–2% smaller than experiments, presumably due to LDA overbinding.

3.2. Constitutional defects at $T=0$ K

At $T=0$ K, the point defect structure of B2 PdIn is solely governed by enthalpy and the point defects at this temperature are referred to as constitutional defects. In Fig. 2, the predicted formation enthalpies of B2 PdIn containing each of the four possible types of constitutional point defects, Va_{Pd} , Va_{In} , Pd_{In} and In_{Pd} , are plotted as four branches, respectively. The off-stoichiometric B2 PdIn alloys were simulated using both 16-atom and 32-atom supercells. Here we consider a canonical ensemble containing a total one mole of In and Pd atoms. Since deviation from stoichiometry can be accommodated by either constitutional antisites or constitutional vacancies, there are two branches in Fig. 2 on either side of the

stoichiometric composition, the branch with lower formation enthalpy being the stable one. Fig. 2 thus shows that the stable constitutional point defects in In-rich and Pd-rich B2 PdIn are Pd vacancies and Pd antisites, respectively. This conclusion is in accordance with Chang and Neumann [3–5]. For the purpose of comparison, we also show in Fig. 2 the experimental calorimetry measurements by Bryant and Pratt [35] and Meschel and Kleppa [36]. As shown, the formation enthalpies of B2 PdIn alloys were underestimated in our calculations by ~ 10 kJ/mol. This is atypical of LDA, which usually overpredict the formation enthalpies.

In Fig. 3, we also compare our predicted equilibrium lattice parameters of B2 PdIn with the experimental measurements by Huang et al. [9] and Fort et al. [37]. Again, there are four branches in Fig. 3, each corresponding to one of the four possible types of constitutional point defects: Va_{Pd} , Va_{In} , Pd_{In} and In_{Pd} . Our calculations underestimate the lattice parameters of B2 PdIn by $\sim 1\%$, while the slopes of the two stable branches are in good agreement with experiments.

We note that, calculations were also performed in the present study employing the generalized gradient approximation (GGA). We found that GGA overestimates the lattice parameters by 1–2% and further underestimates the formation enthalpies of B2 PdIn alloys compared to LDA. Similar to the case of InN [38,39], GGA does not offer any advantage over LDA here, neither for lattice parameters nor for formation enthalpies.

3.3. Defects at finite temperatures

Using the Wagner–Schottky model and the defect formation enthalpies in Table 2, we calculated the point defect concentrations in B2 PdIn at $T=1273$ K as a function of composition and the results are plotted in Fig. 4(a). The major defects in B2 PdIn at high temperatures are Pd vacancies on the In-rich side and Pd antisites on the Pd-rich side, most of which are temperature-independent constitutional defects. In Fig. 4(b), we also show the equilibrium concentrations of thermal defects in B2 PdIn, defined as:

$$x_d^t = x_d - x_d^c \quad (7)$$

where x_d^t and x_d^c are the concentration of thermal and constitutional defects of type d , respectively. We have $x_d^c = \chi$ for Pd antisites and $x_d^c = 2\chi$ for Pd vacancies, with $\chi = |x_{Pd} - 0.5|$ being the absolute deviation from stoichiometry. It is noted that, in order to maintain the overall composition of the alloy, the following constraint must be strictly satisfied at all compositions and temperatures:

Table 3
First principles calculated equilibrium lattice parameters of pure elements in their ground state structures

Element	Crystal Structure	Present Study	Experiments [1]
In	Bct	$a=b=3.18 \text{ \AA}$, $c=4.89 \text{ \AA}$, $c/a=1.54$	$a=b=3.25 \text{ \AA}$, $c=4.95 \text{ \AA}$, $c/a=1.52$
Pd	Fcc	$a=b=c=3.85 \text{ \AA}$	$a=b=c=3.89 \text{ \AA}$

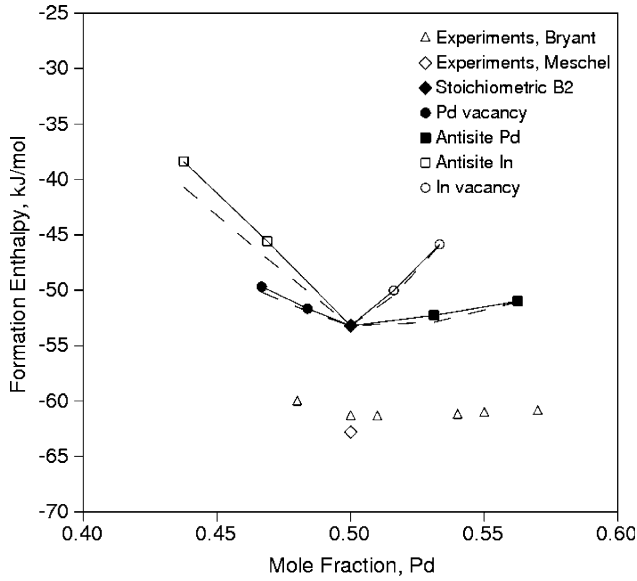


Fig. 2. Comparison between first-principles calculated and experimentally observed formation enthalpies of B2 PdIn as a function of composition. Both results obtained using 16-atom supercells and 32-atom supercells are shown. The solid and dashed lines correspond to unrelaxed and relaxed formation enthalpies, respectively. Experimental data are from Bryant [35] and Meschel and Kleppa [36].

$$2(x_{\text{PdIn}}^t - x_{\text{InPd}}^t) + (x_{\text{VaIn}}^t - x_{\text{VaPd}}^t) = 0 \quad (8)$$

Clearly, the only way to satisfy Eq. (8) is by forming thermal defect complexes. Following are four common types of them:

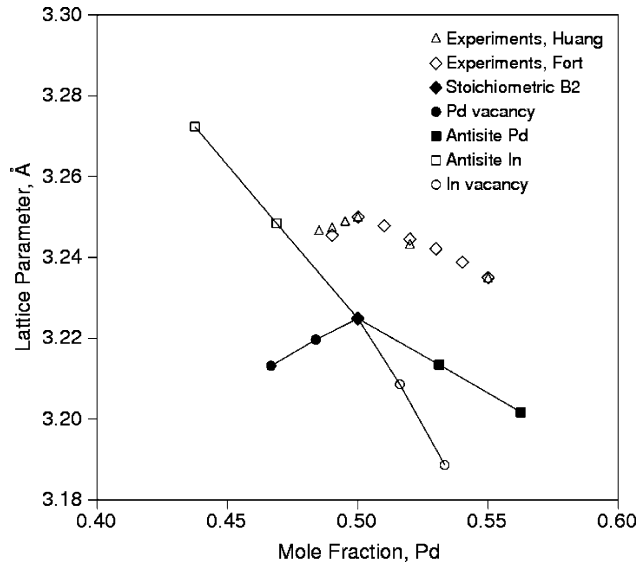
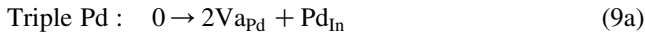


Fig. 3. Comparison between first-principles calculated and experimentally observed equilibrium lattice parameter of B2 PdIn. Both results obtained using 16-atom supercells and 32-atom supercells are shown. Experimental data are from Huang [9] and Fort [37]. (a) Total defect concentrations. (b) Thermal defect concentrations

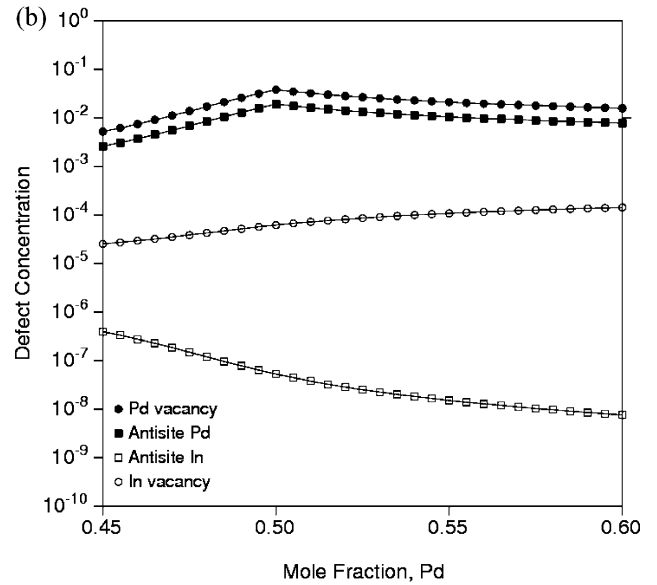
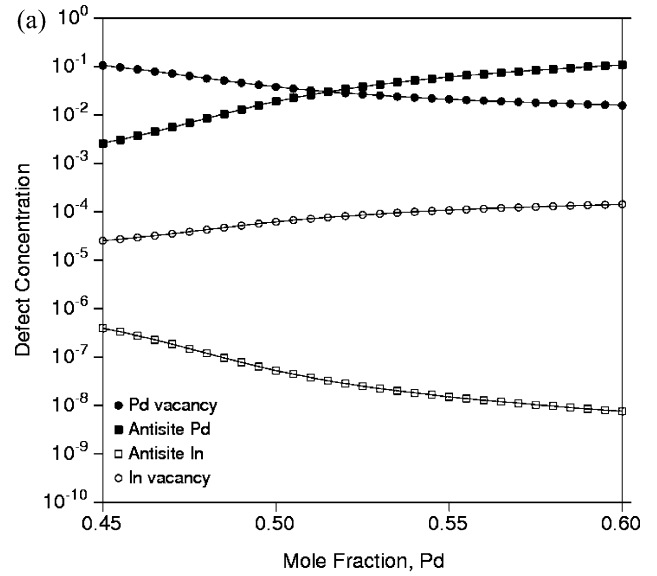
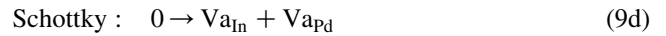
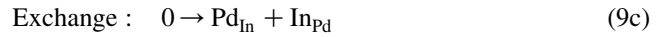
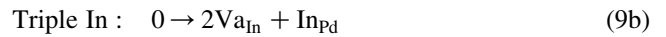


Fig. 4. Equilibrium defect concentrations in B2 PdIn at $T=1273$ K as a function of composition: (a) total defect concentrations and (b) thermal defect concentrations.



According to Fig. 4(b), the major thermal defects in B2 PdIn at high temperatures are Pd vacancies and Pd antisites, the concentrations of which are highest at the stoichiometric composition. The ratio $x_{\text{VaPd}}^t/x_{\text{PdIn}}^t$ is also maintained around 2 over the whole composition range. In contrast, the concentration of In vacancies is low even at high temperatures. Our calculations thus suggest that

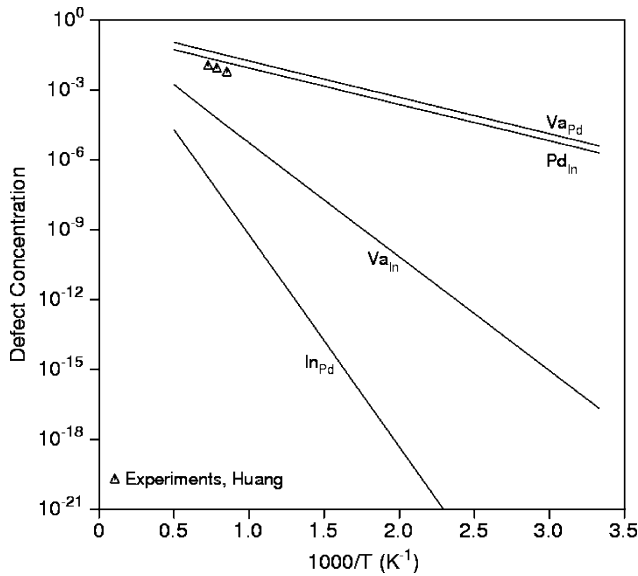


Fig. 5. Arrhenius plot of equilibrium point defect concentrations in stoichiometric B2 PdIn in comparison with experimental vacancy concentration data from Huang et al. [9,10].

the predominant thermal defects in B2 PdIn are of triple-Pd type as proposed by Huang et al. [9,10] and not of Schottky type as proposed by Collins and Sinha [12]. Unlike B2 NiAl, in which the thermal defects are of triple-defect type on the Ni-rich side but are of interbranch type on the Al-rich side [15], the thermal defects in B2 PdIn are of triple-defect type on both sides of stoichiometry.

By transferring Pd atoms from the Pd sublattice to In vacancies on the In sublattice, the Schottky defects can be converted into triple defects via the reaction: $Va_{In} + Va_{Pd} + Pd_{Pd} \rightarrow 2Va_{Pd} + Pd_{In}$. Assuming the point defects to be non-interacting, the formation enthalpies of all four common types of thermal defect complexes were calculated using the formation enthalpies of isolated point defects and the results are also shown in Table 2. As can be seen, our calculations using both 16-atom and 32-atom supercells, with or without local atomic relaxations, consistently show that triple defects have lower formation enthalpy than Schottky defects. Also, since converting Schottky defects into triple defects will produce more point defects and thus more configurational entropy, the triple defects will be further favored with increasing temperature. In other words, the predominance of triple defects over Schottky defects in B2 PdIn is not only energetically favorable, but is also entropically favorable.

Finally, in Fig. 5, we plot our predicted equilibrium point defect concentrations in stoichiometric B2 PdIn as a function of temperature together with the experimental data by Huang et al. [9,10]. It can be seen that triple defects dominate at all temperatures. It can also be observed that our predicted vacancy concentrations are always larger than experimental measurements. One possible reason for such discrepancy is that, since the formation enthalpies were

underestimated in our calculations, it is likely that the defect formation enthalpies were also underestimated. Additionally, since only ideal entropy of mixing was considered in our calculations, the neglect of the role of vibrational entropies in our calculations can also be a factor for such discrepancy.

4. Summary

In the present study, we obtained the formation enthalpies of isolated point defects in stoichiometric B2 PdIn by means of first-principles supercell calculations. Our results show that Pd vacancies and Pd antisites are the constitutional point defects in In-rich and Pd-rich B2 PdIn, respectively. Using the Wagner-Schottky model, we also calculated the thermal defect concentrations at finite temperatures. Our results suggest that the predominant thermal defects in B2 PdIn are triple-Pd defects and not Schottky-type defects.

Acknowledgements

This work is funded by the National Science Foundation through grants DMR-9983532, DMR-0122638, and DMR-0205232. The Materials Simulation Center (MSC) at Penn State led by Dr. Jorge Sofo is acknowledged for the computer resources for first-principles calculations.

References

- [1] White CET, Okamoto H. Phase diagrams of indium alloys and their engineering applications. Materials Park, OH: ASM International; 1991 p. 207–210.
- [2] Bradley AJ, Taylor A. Proc R Soc London, Ser A 1937;159:56.
- [3] Neumann JP, Chang YA. Metall Trans A 1976;7A:1291–3.
- [4] Neumann JP, Chang YA. Acta Materialia 1976;24:593–604.
- [5] Chang YA, Neumann JP. Prog Solid State Chem 1982;14:221.
- [6] Lautenschlager EP, Kiewit DA, Brittain JO. Trans AIME 1965;233: 1297.
- [7] Baker I. Mater Sci Eng A 1995;193:1–13.
- [8] Mishin Y, Lozovoi AY, Alavi A. Phys Rev B 2003;67:014201.
- [9] Huang M, Xie F, Yan X, Chang YA. Intermetallics 2001;9:457–60.
- [10] Huang M, Oates WA, Chang YA. Philos Mag 2003;83:589–601.
- [11] Jiang C, Liu ZK. Metall Trans A 2002;33:3597–603.
- [12] Collins GS, Sinha P. Hyperfine Interact 2000;130:151–79.
- [13] Kohn W, Sham L. Phys Rev A 1965;140:1133.
- [14] Wagner C, Schottky W. Z Physik Chem B 1930;11:163.
- [15] Korzhavyi PA, Ruban AV, Lozovoi AY, Vekilov YK, Abrikosov IA, Johansson B. Phys Rev B 2000;61:6003–18.
- [16] Fu CL, Zou J. Acta Mater 1996;44:1471–8.
- [17] Fu CL, Ye YY, Yoo MH, Ho KM. Phys Rev B 1993;48:6712.
- [18] Fu CL. Phys Rev B 1995;52:3151.
- [19] Meyer B, Fahnle M. Phys Rev B 1999;59:6072.
- [20] Song Y, Guo ZX, Yang R, Li D. Acta Mater 2001;49:1647–54.
- [21] Medvedeva NI, Gornostyrev YN, Novikov DL, Mryasov ON, Freeman AJ. Acta Mater 1998;46:3433–42.

- [22] Parlinski K, Jochym PT, Kozubski R, Oramus P. *Intermetallics* 2003; 11:157–60.
- [23] Jiang C, Besser MF, Sordélet DJ, Gleeson B. *Acta Mater* 2005;53: 2101–9.
- [24] Djajaputra D, Cooper BR. *Phys Rev B* 2001;64:085121.
- [25] Kellou A, Feraoun HI, Grosdidier T, Coddet C, Aourag H. *Acta Mater* 2004;52:3263–71.
- [26] Vanderbilt D. *Phys Rev B* 1990;41:7892–5.
- [27] Kresse G, Hafner J. *J Phys -Condens Matter* 1994;6:8245–57.
- [28] Kresse G, Furthmuller J. *Phys Rev B* 1996;54:11169–86.
- [29] Kresse G, Furthmuller J. *Comput Mater Sci* 1996;6:15–50.
- [30] Ceperley DM, Alder BJ. *Phys Rev Lett* 1980;45:566.
- [31] Monkhorst HJ, Pack JD. *Phys Rev B* 1972;13:5188.
- [32] Lozovoi AY, Ponomarev KV, Vekilov YK, Korzhavyi PA, Abrikosov IA. *Phys Solid State* 1999;41:1494–9.
- [33] Simak SI, Haussermann U, Ahuja R, Lidin S, Johansson B. *Phys Rev Lett* 2000;85:142–5.
- [34] Mikhaylushkin AS, Haussermann U, Johansson B, Simak SI. *Phys Rev Lett* 2004;92:195501.
- [35] Bryant AW, Pratt JN. *Colloque sur la thermochimie* 1972;201:241–7.
- [36] Meschel SV, Kleppa OJ. *J Alloys Compd* 2002;333:91–8.
- [37] Fort D, Smallman RE, Harris IR. *J Less-Common Met* 1973;31: 263–79.
- [38] Stampfl C, Van de Walle CG. *Phys Rev B* 1999;59:5521.
- [39] Zoroddu A, Bernardini F, Ruggerone P, Fiorentini V. *Phys Rev B* 2001;64:045208.